

Quantum chemical computational studies on bis-thiourea zinc acetate

HACER PIR¹, NERGIN GÜNAY¹, ÖMER TAMER¹, DAVUT AVCI¹,
ERDOĞAN TARCAN², YUSUF ATALAY^{1*}

¹Sakarya University, Art and Science Faculty, Department of Physics, 54187, Sakarya, Turkey

²Kocaeli University, Department of Physics, Kocaeli, Turkey

In this study, quantum chemical calculations of vibrational spectra, Raman spectra, electronic properties (total energy, dipole moment, electronegativity, chemical hardness and softness), Mulliken atomic charges and thermodynamic parameters of bis-thiourea zinc acetate (BTZA) have been performed using Gaussian 09 program. Additionally, nonlinear optical (NLO), conformational, natural bond orbital (NBO) analyses of BTZA have been carried out using the same program. The structural and spectroscopic data of the molecule in the ground state have been calculated using Hartree-Fock (HF) and density functional method (DFT/B3LYP) with the 6-311++G(d,p) basis set. In addition, the molecular frontier orbital energies (HOMO, HOMO-1, LUMO and LUMO+1) of the title compound have been calculated at the HF and B3LYP levels. The calculated HOMO and LUMO energies show that charge transfer occurs within the molecule. Finally, the calculated results were applied to simulate infrared and Raman spectra of the title compound which showed good agreement with the experimental ones.

Keywords: *bis-thiourea zinc acetate (BTZA); IR and NMR spectra; DFT and HF calculations; NLO and NBO analyses, conformational analysis*

© Wrocław University of Technology.

1. Introduction

Thiourea, also known as Antu, is an organic compound of carbon, nitrogen, sulfur and hydrogen, with the formula CSN₂H₄ or (NH₂)₂CS. It is similar to urea, except that the oxygen atom is replaced by a sulfur atom. The properties of urea and thiourea differ significantly because of the differences in relative electronegativities of sulfur and oxygen. Thiourea is a versatile reagent in organic synthesis. Thiourea is a planar molecule and a centrosymmetric molecule; when coordinated with metal ions it becomes non centrosymmetric material, exhibiting non-linear optical activity [1]. Thiourea and its family of crystals have been reported to be of very great interest for the non-linear optical (NLO) applications [2–5]. Recently, zinc thiourea chloride single crystals have been grown and their structural and optical properties have been reported [6]. The single crystals of

bis-thiourea zinc acetate (BTZA) were grown under optimized growth conditions by D. Jayalakshmi et al. [7, 8].

Density functional theory (DFT), namely, the B3LYP method yields sufficiently good and consistent results even with the standard 6-31G* basis set at moderate computational costs. Especially, results obtained from calculations of the structural and spectroscopic properties provide excellent agreement with the experimental results. Recently, vibrational properties of different materials have been reported [9–14]. This type of theoretical vibration studies is therefore very important.

In a previous publication, bis-thiourea zinc acetate (BTZA) was synthesized by D. Jayalakshmi et al. and its spectroscopic (FT-IR and FT-Raman) and non-linear optical properties were investigated [15]. In spite of its importance, mentioned above, there is no theoretical calculation on the BTZA in literature. Therefore, we have performed a deep investigation and carried out the theoretical calculations using conformational, natural

*E-mail: yatalay@sakarya.edu.tr

bond orbital (NBO) and nonlinear optical (NLO) analyses. IR and Raman spectra, molecular electrostatic potential maps (MEP) and molecular surfaces, Mulliken charges, as well as electronic and thermodynamic properties of the title compound have been studied. The evaluations have been performed by means of the HF/6-311++G(d,p) and DFT/B3LYP/6-311++G(d,p) levels of theory. Also, the chemical hardness (η) and softness (S) as well as electronegativity (χ) parameters have been obtained by using frontier molecular orbital energies at DFT/6-311++G(d,p) level.

2. Computational details

The molecular structure of BTZA in the ground state (in vacuo) was computed by performing both Hartree-Fock (HF) and the density functional theory (DFT) calculations by hybrid B3LYP functional (Becke's three-parameter hybrid model using the Lee-Yang Parr correlation functional) methods [16, 17] at 6-311++G(d,p) level. The theoretical geometric structure of the title compound is given in Fig. 1b. The calculations of optimized geometrical structure, using conformational, natural bond orbital (NBO) and nonlinear optical (NLO) analyses, IR and Raman spectra, dipole moments and frontier molecular orbitals, Mulliken atomic charge, molecular electrostatic potential and thermodynamic properties of the title compound in this study were carried out by using Gaussian 09W program package [18] and Gauss-View molecular visualization program [19]. Additionally, harmonic vibrational frequencies for the title compound were calculated by these methods and then scaled by 0.90 and 0.96 [20] and finally compared with the experimental data.

3. Results and discussion

3.1. Assignments of the vibrational modes

The title compound was synthesized by D. Jayalakshmi *et al.*, and its molecular structure with numbering of atoms is shown in Fig. 1a [15]. The optimized geometric structure of BTZA has been calculated at HF/6-311++G(d,p) and B3LYP/6-

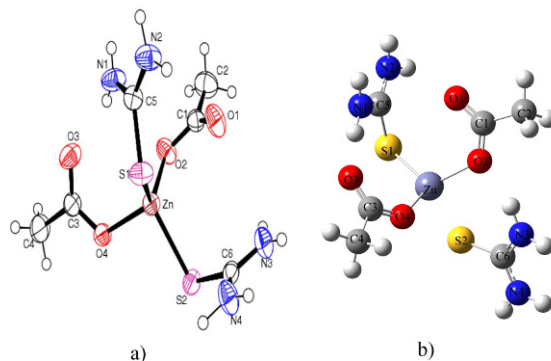


Fig. 1. BTZA structure a) experimental [15], b) the optimized geometric structure obtained at B3LYP/6-311++G(d,p) level.

311++G(d,p) levels of theory. The theoretical geometric structure of the title compound is shown in Fig. 1b.

D. Jayalakshmi *et al.* investigated the Raman and infrared spectra of the title compound experimentally, and assigned vibrational modes [15]. We have simulated the theoretical vibrational spectra of the title compound by using B3LYP and HF method with 6-311++G(d,p) basis set. None of the predicted vibrational spectra had an imaginary frequency proving that the optimized geometry was located at the lowest point on the potential energy surface. However, slight differences could be observed between the experimental and theoretical vibrational wavenumbers (Table 1). The reason of these differences can be attributed to the fact that the calculations were performed in gas phase, while the experimental process was performed in solid phase.

The group of bands in the 3500 – 3300 cm^{-1} [15] region in the infrared and Raman spectra of both compounds can be assigned to asymmetric N–H stretching modes, and these bands were calculated in the range of 3527 – 3446 and 3564 – 3463 cm^{-1} for HF and DFT/B3LYP levels, respectively. The C–H stretching bands were calculated around 2926 – 2834 cm^{-1} and 3017 – 2915 cm^{-1} using HF and B3LYP method, respectively with 6-311++G(d,p) basis set, and these bands were observed at the same region in

Table 1. Comparison of the calculated vibrational wavenumbers and assignments for BTZA.

Assignments	Exp. [15]	Calculated	
		HF/6-311++G(d,p)	B3LYP/6-311++G(d,p)
$\nu_a(\text{N-H})$	3263	3527	3564
$\nu_a(\text{N-H})$	–	3446	3463
$\nu_s(\text{N-H})$	–	3406	3442
$\nu_s(\text{N-H})$	–	3112	3429
$\nu_a(\text{C-H}_3)$	2904	2926	3017
$\nu_a(\text{C-H}_3)$	–	2886	2971
$\nu_s(\text{C-H}_3)$	–	2840	2920
$\nu_s(\text{C-H}_3)$	–	2834	2915
$\nu(\text{C=O}), \beta(\text{N-H}_2)$	1631	1665	1647
$\nu(\text{C=O}), \beta(\text{N-H}_2)$	1611	1657	1639
$\beta(\text{N-H}_2), \nu(\text{C=O})$	–	1653	1630
$\beta(\text{N-H}_2), \nu(\text{C=O})$	–	1616	1595
$\beta(\text{N-H}_2), \nu(\text{C=O})$	–	1605	1578
$\beta(\text{N-H}_2), \nu(\text{C=O})$	–	1598	1568
$\nu(\text{N=C-N})$	1500	1470	1488
$\nu(\text{N=C-N})$	1491	1439	1451
$\beta(\text{C-H}_3)$	1415	1429	1425
$\beta(\text{C-H}_3)$	–	1427	1421
$\beta(\text{C-H}_3)$	–	1415	1412
$\nu(\text{C-C}), \beta(\text{C-H}_3)$	–	1413	1407
$\beta(\text{C-H}_3)$	–	1411	1369
$\tau(\text{C-H}_3), \nu(\text{C=O}), \beta(\text{N=C-N})$	–	1383	1349
$\tau(\text{C-H}_3), \nu(\text{C=O}), \beta(\text{N=C-N})$	–	1376	1347
$\beta(\text{N-H}_2)$	1338	1368	–
$\tau(\text{C-H}_3)$	1303	1323	1332
$\tau(\text{C-H}_3)$	–	1304	1311
$\tau(\text{C-H}_3), \nu(\text{C-O})$	–	–	1271
$\beta(\text{N-H}_2)$	–	1085	1084
$\beta(\text{N-H}_2)$	–	1073	1074
$\beta(\text{N-H}_2)$	–	1064	1059
w(C-C)	1041	1046	1032
w(C-C)	–	1043	1022
w(N-H ₂)	–	1040	1019
w(C-H ₃)	933	1006	994
w(C-H ₃)	–	999	985
$\nu(\text{C-C})$	–	908	914
$\nu(\text{C-C})$	–	904	893
w(N-H ₂)	779	818	890
w(N-H ₂)	–	762	816
$\beta(\text{N=C=N}), \nu(\text{C-S})$	678	686	702

Table 1. (Continuation) Comparison of the calculated vibrational wavenumbers and assignments for BTZA.

Assignments	Exp. [15]	Calculated	
		HF/6-311++G(d,p)	B3LYP/6-311++G(d,p)
β (N=C=N), ν (C-S)	–	679	685
w(N=C=N)	–	665	641
ν (C-C), β (O=C=O)	613	643	636
ν (C-C), β (O=C=O)	–	637	634
w(N=C=N)	–	621	601
w(C-H ₃)	–	608	593
w(C-H ₃)	–	604	587
w(N-H ₂)	530	521	516
w(N-H ₂)	–	510	500
ν (O-Zn)	–	493	483
ν (O-Zn)	–	481	477
w(N-H ₂)	482	475	468
β (N=C-N)	–	460	461
β (N=C-N)	–	452	412
w(N-H ₂)	–	408	394
β (N=C-N)	–	403	371
β (N=C-N)	–	386	353
w(N-H ₂)	–	373	283
ν (O-Zn-O)	–	273	259
ν (O-Zn)	–	253	226
w(N-H ₂)	–	227	216
Lattice	–	211	205
Lattice	–	184	181
Lattice	–	162	175
Lattice	–	158	153
Lattice	–	145	139

ν , stretching; a, asymmetric; s, symmetric; β , in-plane bending; w, out of plane bending; t, twisting; τ , torsion.

the FT-IR spectrum [15]. Additionally, symmetric and asymmetric vibration modes of N-H and C-H₃ are pure modes, as can be inferred from Table 1. The C-S bending mode was observed at 730 – 713 cm⁻¹ [15], these bands were calculated at 686 – 679 cm⁻¹ and 702 – 685 cm⁻¹ using HF and B3LYP methods, with 6-31++G(dp) basis set. The Raman stretching vibration bands were observed at 500 cm⁻¹ and at 480 cm⁻¹ for C-S and Zn-Cl, respectively. The peaks at 1611 and 1631 cm⁻¹ with very strong intensity in the FTIR spectrum

could be assigned to NH₂ bending vibrations. The corresponding bands also appeared at 1581 and 1643 cm⁻¹ [15] in the Raman spectrum. These bands were calculated at 1665 and 1657 cm⁻¹ using HF method and 1647 and 1639 cm⁻¹ using B3LYP method with 6-31++G(dp) basis set. This mode also appeared at 1338 cm⁻¹ [15], and it was calculated at 1368 cm⁻¹ for HF level. It can be seen in Table 1 that the NH₂ bending modes are mostly coupled with C=O stretching vibrations. The N-C-N stretching vibrations were observed

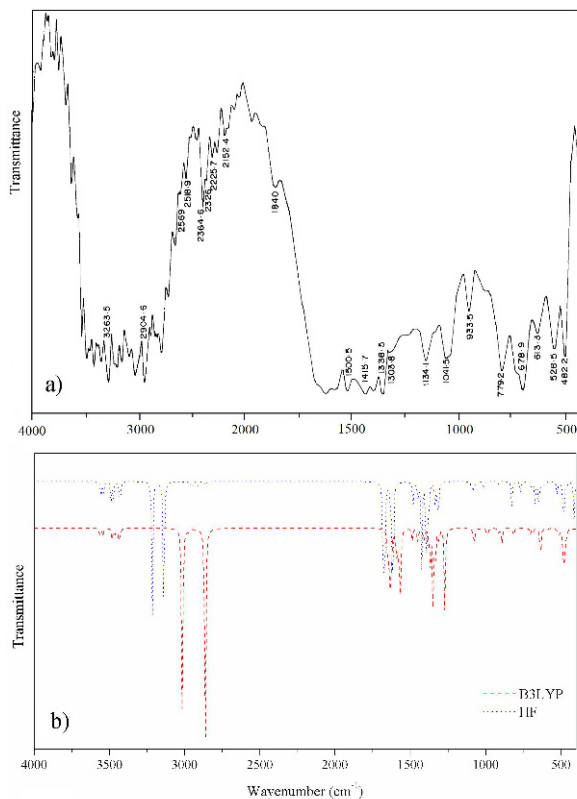


Fig. 2. Spectra of BTZA a) experimental FT-IR spectrum, b) calculated IR spectrum.

at 1500 cm^{-1} [15], these bands were calculated at 1470 and 1439 cm^{-1} using HF method, and 1488 and 1451 cm^{-1} using B3LYP method with 6-31++G(dp) basis set. The C–C out of plane bending vibration was observed at 1041 cm^{-1} , and this mode was predicted as $1046 - 1043\text{ cm}^{-1}$ and $1032 - 1022\text{ cm}^{-1}$ for HF and B3LYP, respectively. The C–H₃ out of plane bending vibration, experimentally observed at 933 cm^{-1} , was calculated at 1006 cm^{-1} for HF and 994 cm^{-1} for B3LYP.

The comparative IR and Raman spectra of the experimental and the calculated HF and DFT spectra are given in Figs. 2 and 3, respectively. As can be seen from Table 1 and Figs. 2 and 3 there is a good agreement between the experimental and theoretical results.

3.2. Conformational analysis

The minimum point structures located on the potential surface scan (PES) of the title com-

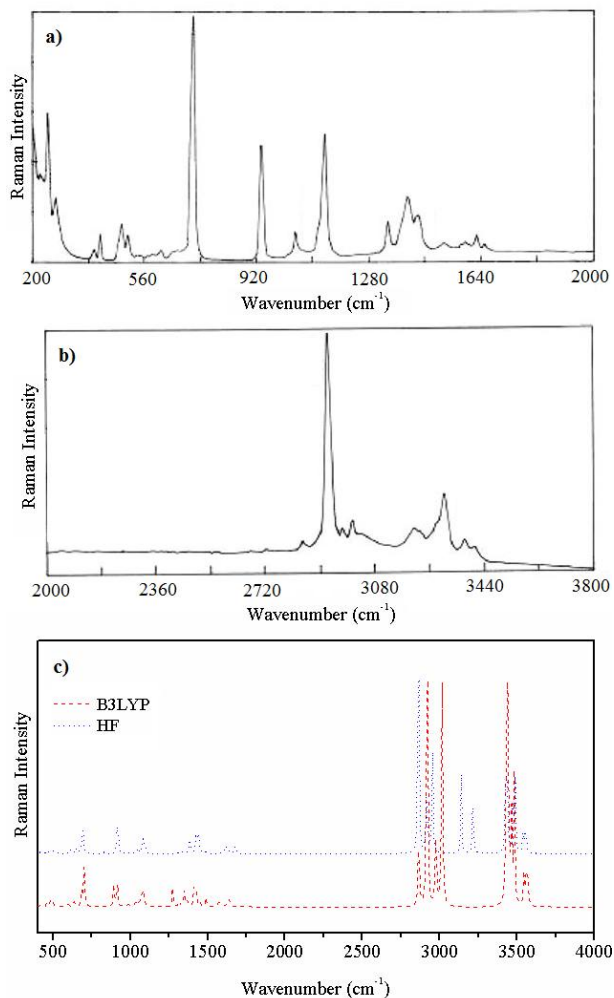


Fig. 3. Experimental FT-Raman spectra of BTZA a) and b), the calculated FT-Raman spectrum of BTZA c).

pound were employed for optimization using PM6. From the rotation of different groups the minimum energy conformation was obtained and valuable structural information about protein was acquired to prepare the basis for the further investigations. In order to reveal all possible conformational structures of BTZA molecule, a detailed potential energy curves for τ_1 (Zn–S₂–C₆–N₃), τ_2 (O₄–Zn–S₂–C₆), τ_3 (S₁–Zn–S₂–C₆), τ_4 (Zn–O₄–C₃–O₃) and τ_5 (O₂–Zn–O₄–C₃) dihedral angles were calculated in steps of 10° and are depicted in Fig. 4. The highest and lowest energy conformers for τ_1 , τ_2 , τ_3 , τ_4 and τ_5 dihedral angles and the computed energy values of these dihedral angles are given in Fig. 4.

The conformers resulting from unconstrained optimizations of the highest and the lowest energy structures of the contour plot of energy surfaces calculated by PM6 for BTZA molecule are shown in Fig. 5.

3.3. Natural Bonding Orbital (NBO) analysis

NBO calculations have been performed using Gaussian 09W program package [18] and GaussView molecular visualization program [19] at the PM6 in order to understand various second-order interactions between the filled orbitals of one subsystem and vacant orbitals of another subsystem, which are a measure of the intermolecular delocalization or hyperconjugation. A useful aspect of the NBO method is that it gives information about interactions in both filled and virtual orbital spaces, which could enhance the analysis of intra and intermolecular interactions. The second-order Fock matrix was used to evaluate the donor-acceptor interactions in the NBO basis [21]. The interactions result in a loss of occupancy from the localized NBO of the idealized Lewis structure into an empty non-Lewis orbital. For each donor (i) and acceptor (j), the stabilization energy $E(2)$ associated with the delocalization $i \rightarrow j$ is estimated as [22]:

$$E(2) = \Delta E_{ij} = q_i \frac{F(i, j)^2}{\epsilon_j - \epsilon'_i} \quad (1)$$

where q_i is the donor orbital occupancy, ϵ_i and ϵ_j are diagonal elements and $F(i, j)$ is the off-diagonal NBO Fock matrix element. Hybrids of natural bond orbitals for the title compound, calculated by NBO analysis, are given in Table 2. In NBO analysis large $E(2)$ value shows the intensive interaction between electron-donors and electron-acceptors. This large $E(2)$ value indicates the greater extent of conjugation in the whole system. The possible intensive interactions are given in Table 1. In NBO analysis, the hyperconjugative $\sigma \rightarrow \sigma^*$ interactions play a highly important role. These interactions represent the weak departure from a strictly localized natural Lewis structure that constitutes the primary “noncovalent” effects. The results of NBO analysis tabulated in Ta-

ble 2 indicate that there is a strong hyperconjugative interaction $LP1(S_1) \rightarrow \sigma^*(Zn-S_1)$ and $\sigma(Zn-S_2) \rightarrow \sigma^*(O_4-C_3)$ for the title compound which is equal to 3.01 and 0.95 kcal/mol at HF and 4.02 and 0.32 kcal/mol at B3YLP levels, respectively. The second-order perturbation theory analysis of Fock matrix in NBO basis shows strong intramolecular hyperconjugative interactions of electrons. The interaction energies of $\sigma(C5-N1) \rightarrow \pi^*(C5-N1)$ and $LP1(N4) \rightarrow \sigma^*(C6-N3)$ were calculated as 152.11 and 141.14 kcal/mol at HF and 107.78 and 62.55 kcal/mol at B3LYP level, respectively. These interactions result in intramolecular charge transfer causing stabilization of the title compound.

3.4. Polarizabilities and hyperpolarizabilities

The polarizabilities and hyperpolarizabilities characterize the response of a system in an applied electric field [23, 24]. Electric polarizability is a fundamental characteristic of atomic and molecular systems [25]. Polarizabilities and hyperpolarizabilities could determine not only the strength of molecular interactions (such as the long-range intermolecular induction, dispersion forces, etc.) as well as the cross sections of different scattering and collision processes, but also the nonlinear optical properties (NLO) of the system [26]. The theory of electric polarizability is a key element of the rational interpretation of a wide range of phenomena, from nonlinear optics [27] and electron scattering [28] to phenomena induced by intermolecular interactions [29].

$$E = E^0 - \mu_\alpha F_\alpha - \frac{1}{2} \alpha_{\alpha\beta} F_\alpha F_\beta - \frac{1}{6} \beta_{\alpha\beta\gamma} F_\alpha F_\beta F_\gamma - \frac{1}{24} \gamma_{\alpha\beta\gamma\delta} F_\alpha F_\beta F_\gamma F_\delta + \dots \quad (2)$$

where E^0 is the energy of the free molecule, F_α is the field at the origin and μ_α , $\alpha_{\alpha\beta}$, $\beta_{\alpha\beta\gamma}$ and $\gamma_{\alpha\beta\gamma\delta}$ are the components of dipole moment, polarizability and the first-order hyperpolarizabilities, respectively. In this paper, we present the values of the total static dipole moment (μ), the mean polarizability ($\langle \alpha \rangle$), the anisotropy of the polarizability ($\Delta\alpha$) and the mean first-order hyperpolarizability

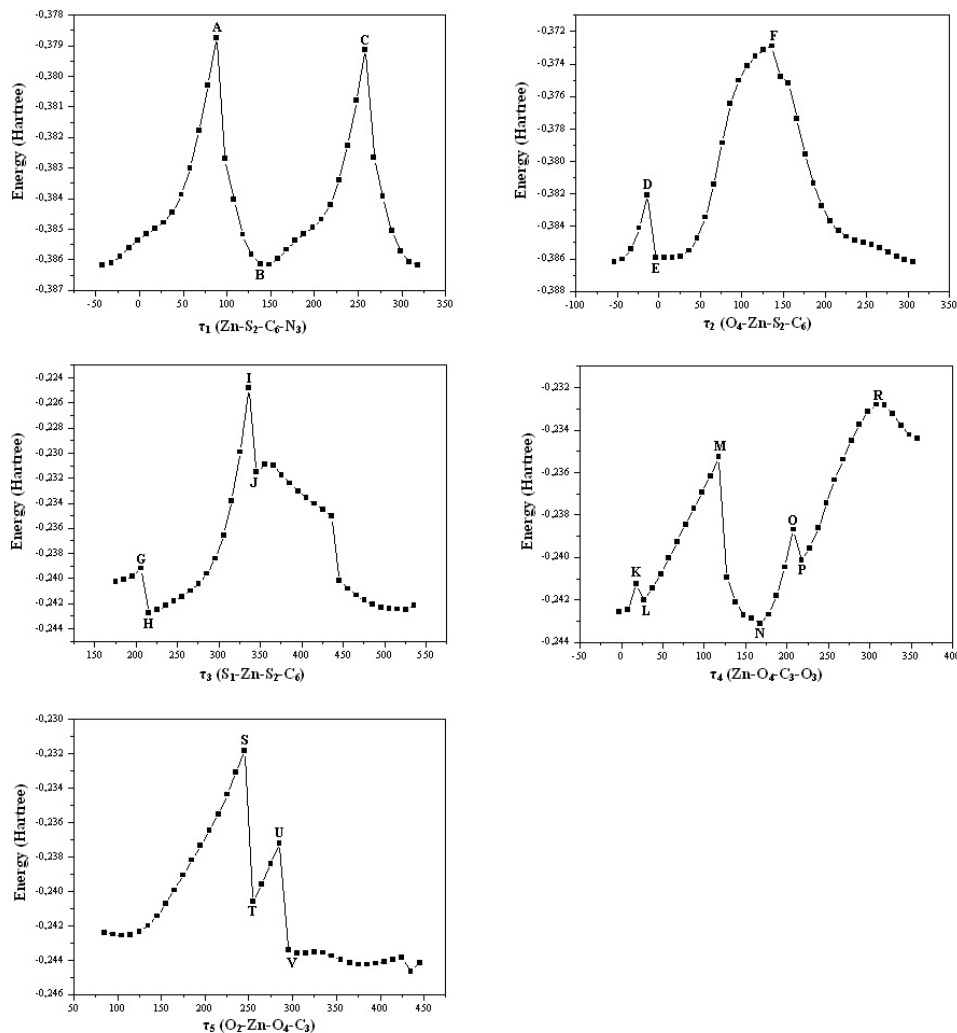


Fig. 4. One-dimensional potential energy surface (PES) scans of the energies of BTZA vs. dihedral angles (τ), calculated using PM6.

$\langle\beta\rangle$ as defined in [30] by the following equations [31, 32]:

$$\mu = (\mu_x^2 + \mu_y^2 + \mu_z^2)^{\frac{1}{2}} \quad (3)$$

where

$$\langle\alpha\rangle = \left(\frac{\alpha_{xx} + \alpha_{yy} + \alpha_{zz}}{3} \right) \quad (4)$$

$$\Delta\alpha = \left(\frac{(\alpha_{xx} - \alpha_{yy})^2 + (\alpha_{yy} - \alpha_{zz})^2 + (\alpha_{zz} - \alpha_{xx})^2}{2} \right)^{\frac{1}{2}} \quad (5)$$

$$\langle\beta\rangle = (\beta_x^2 + \beta_y^2 + \beta_z^2)^{\frac{1}{2}} \quad (6)$$

$$\begin{aligned} \beta_x &= \beta_{xxx} + \beta_{xyy} + \beta_{xzz} \\ \beta_y &= \beta_{yyy} + \beta_{xxy} + \beta_{yzz} \\ \beta_z &= \beta_{zzz} + \beta_{xxz} + \beta_{yyz} \end{aligned} \quad (7)$$

The total static dipole moment, the mean polarizability, the anisotropy of the polarizability ($\Delta\alpha$) and the mean first-order hyperpolarizability ($\langle\beta\rangle$) have been calculated for BTZA molecule using Hartree-Fock (HF) and density functional method

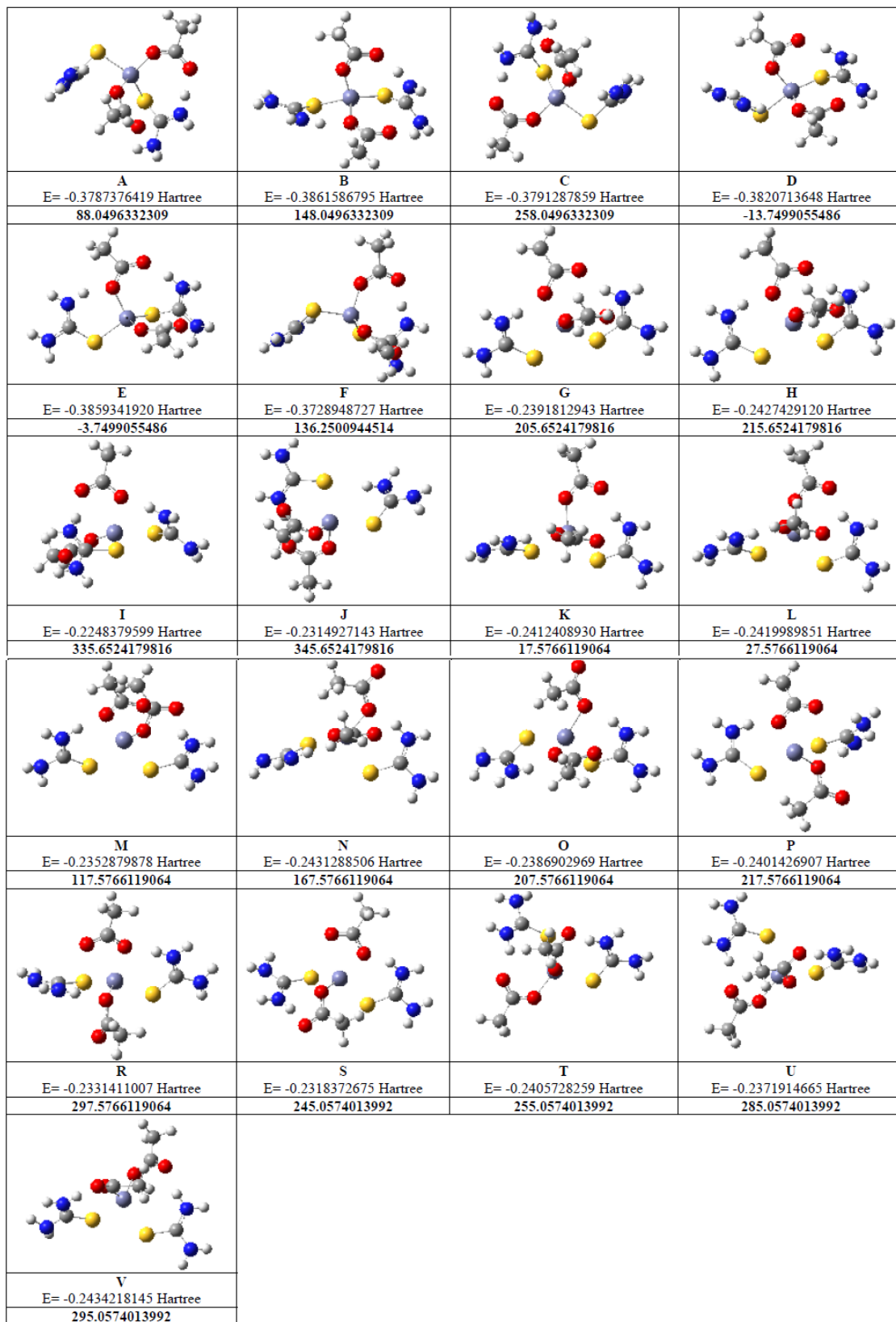


Fig. 5. The highest and lowest energy conformations of BTZA calculated using PM6.

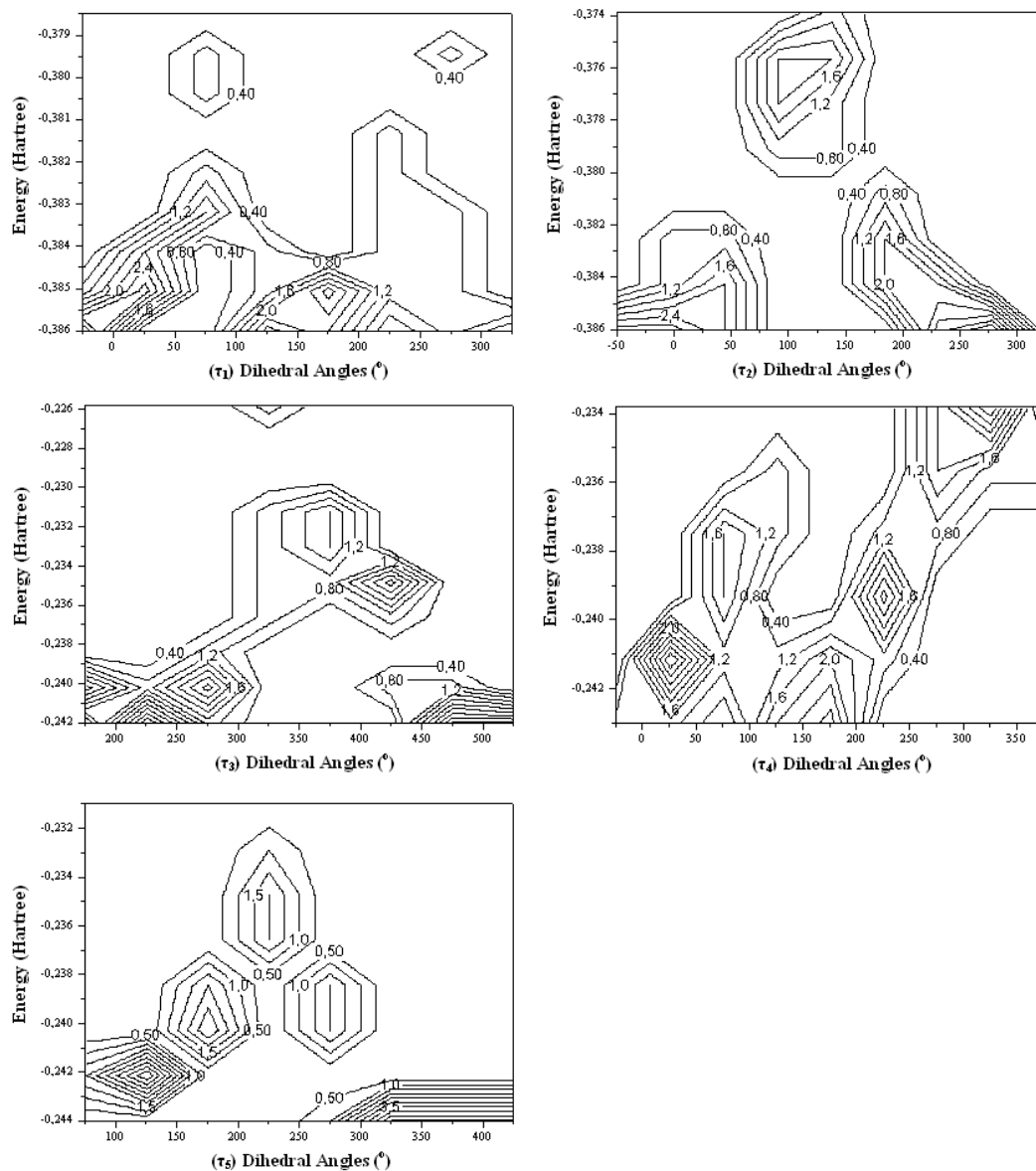


Fig. 6. Contour plots of energy surfaces of BTZA calculated using PM6.

(DFT/B3LYP) with the 6-311++G(d,p) basis set. The α , β and γ components of GAUSSIAN 09W output are reported in atomic units and therefore the calculated values are converted into electrostatic units (α : 1 a.u. = 0.1482×10^{-24} esu and β : 1 a.u. = 8.6393×10^{-33} esu) and given in Table 3.

A dipole moment in a molecule is an important property since it can be used as an indicator of the charge movement across the molecule.

The direction of dipole moment depends on the positive and negative charge centers. The dipole moment of the title compound was calculated as 7.2060 and 6.5080 Debye at HF and B3LYP levels, respectively. From Table 3, the maximum contribution to the dipole moment is from x direction, while the contribution from z direction to the dipole moment is minimum. According to the present calculations shown in Table 3, the $\Delta\alpha$, $\langle\alpha\rangle$ and $\langle\beta\rangle$ values are pre-

Table 2. Second-order perturbation theory analysis of Fock matrix in NBO basic corresponding to the intermolecular bonds of BTZA.

Donor (i)	ED(i) (e)		Acceptor (j)	ED(j) (e)		E(2) ^a (kcal/mol)		E(j)-E(i) ^b (a.u.)		F(i,j) ^c (a.u.)	
	HF	B3LYP		HF	B3LYP	HF	B3LYP	HF	B3LYP	HF	B3LYP
σ (Zn-S ₁)	1.89183	1.86366	σ^* (Zn-S ₁)	0.07990	0.10944	1.64	1.67	0.78	0.50	0.032	0.026
σ (Zn-S ₁)	1.89183	1.86366	σ^* (Zn-S ₂)	0.11387	0.18046	3.45	5.13	0.78	0.49	0.046	0.045
σ (Zn-S ₁)	1.89183	1.86366	σ^* (S ₁ -C ₅)	0.02036	0.02767	1.15	0.65	0.96	0.60	0.030	0.018
σ (Zn-S ₁)	1.89183	1.86366	σ^* (C ₅ -N ₁)	0.12410	0.09650	1.69	0.81	1.37	0.81	0.043	0.023
σ (Zn-S ₁)	1.89183	1.86366	π^* (C ₅ -N ₁)	0.18329	0.40983	3.55	9.86	1.38	0.41	0.064	0.061
σ (Zn-S ₂)	1.83244	1.74237	σ^* (Zn-S ₂)	0.11387	0.18046	2.49	2.32	0.67	0.39	0.037	0.027
σ (Zn-S ₂)	1.83244	1.74237	σ^* (S ₂ -C ₆)	0.02077	0.02811	3.04	2.21	0.87	0.50	0.048	0.032
σ (Zn-S ₂)	1.83244	1.74237	σ^* (C ₆ -N ₄)	0.03243	0.03814	2.96	0.97	1.15	0.71	0.054	0.025
σ (S ₁ -C ₅)	1.97332	1.97218	σ^* (Zn-S ₁)	0.07990	0.10944	1.17	1.15	1.13	0.79	0.033	0.027
σ (S ₂ -C ₆)	1.97494	1.97465	σ^* (Zn-S ₂)	0.11387	0.18046	2.69	3.18	1.17	0.81	0.051	0.047
σ (C ₅ -N ₁)	1.85549	1.98681	σ^* (C ₅ -N ₁)	0.12410	0.09650	2.56	0.84	1.61	1.25	0.058	0.029
σ (C ₅ -N ₁)	1.85549	1.98681	π^* (C ₅ -N ₁)	0.18329	0.40983	152.11	141.14	1.62	0.85	0.448	0.034
π (C ₆ -N ₃)	1.99194	1.99111	σ^* (C ₆ -N ₄)	0.03243	0.03814	0.56	0.51	1.93	1.33	0.030	0.023
π (C ₆ -N ₃)	1.99194	1.99111	σ^* (C ₆ -N ₃)	0.42299	0.52768	0.68	0.61	1.26	0.84	0.029	0.023
LP6* (Zn)	0.13434	0.17544	σ^* (S ₂ -C ₆)	0.02077	0.02811	0.62	0.60	0.20	0.10	0.035	0.022
LP1 (S ₁)	1.95390	1.94979	σ^* (Zn-S ₁)	0.07990	0.10944	3.01	4.02	0.95	0.69	0.048	0.048
LP1 (S ₁)	1.95390	1.94979	σ^* (C ₅ -N ₁)	0.12410	0.09650	7.46	7.38	1.54	1.01	0.098	0.078
LP2 (S ₁)	1.87920	1.83343	π^* (C ₅ -N ₁)	0.18329	0.40983	5.97	10.46	1.28	0.31	0.079	0.055
LP1 (N ₄)	1.77170	1.74380	σ^* (C ₆ -N ₃)	0.42299	0.52768	107.78	62.55	0.50	0.24	0.219	0.118
σ^* (C ₆ -N ₃)	0.42299	0.52768	σ^* (Zn-S ₂)	0.11387	0.18046	2.24	1.73	0.19	0.18	0.035	0.026
σ^* (C ₆ -N ₃)	0.42299	0.52768	π^* (C ₆ -N ₃)	0.03529	0.05057	1.44	4.47	0.69	0.52	0.059	0.080
σ (Zn-S ₂)	1.83244	1.74237	σ^* (O ₄ -C ₃)	1.99564	1.99564	0.95	0.32	0.60	0.79	0.074	0.015

^a E(2) means energy of hyperconjugative interactions (stabilization energy).

^b Energy difference between donor and acceptor i and j NBO orbitals.

^c F(i, j) is the Fock matrix element between i and j NBO orbitals.

dicted as 6.4314×10^{-24} esu, 24.1478×10^{-24} esu and 993.7770×10^{-33} esu at HF level, while 8.6123×10^{-24} esu, 28.5050×10^{-24} esu and $2563.0756 \times 10^{-33}$ esu at B3LYP level.

3.5. Frontier molecular orbitals (FMOs)

The highest occupied molecular orbital (HOMO) and the lowest unoccupied molecular orbital (LUMO) are the main orbitals taking part in a chemical reaction. The HOMO energy characterizes the ability of electron giving, the LUMO characterizes the ability of electron accepting, and the gap between HOMO and LUMO characterizes

the molecular chemical stability [33]. The total energy, HOMO and LUMO energies, the energy gap (ΔE), the ionization potential (I), the electron affinity (A), the absolute electronegativity (χ), the absolute hardness (η) and softness (S) for BTZA molecule has been calculated at HF and DFT(B3LYP) level in the 6-311++G(d,p) basis set. From Table 4, the HOMO and LUMO energies of the title compound are predicted as -9.3638 and 0.5197 eV at HF level, and -6.4037 and -1.0514 eV at B3LYP level. These HOMO and LUMO energies show that charge transfer occurs within the molecule.

Table 3. Longitudinal component of the total static dipole moment (μ), the mean polarizability ($\langle\alpha\rangle$), the anisotropy of the polarizability ($\Delta\alpha$) and the mean first hyperpolarizability ($\langle\beta\rangle$) of BTZA.

Property	HF/6-311++G(d,p)	B3LYP/6-311++G(d,p)
μ_x	-5.5635 Debye	-5.0138 Debye
μ_x	-3.8835 Debye	-3.7289 Debye
μ_x	2.4272 Debye	1.8198 Debye
μ	7.2060 Debye	6.5080 Debye
α_{xx}	191.8713 a.u.	231.0270 a.u.
α_{yy}	148.3793 a.u.	174.8003 a.u.
α_{zz}	148.5705 a.u.	171.1965 a.u.
$\langle\alpha\rangle$	162.9404 a.u.	192.3412 a.u.
$\langle\alpha\rangle$	24.1478×10^{-24} esu	28.5050×10^{-24} esu
$\Delta\alpha$	43.3967 a.u.	58.1125 a.u.
$\Delta\alpha$	6.4314×10^{-24} esu	8.6123×10^{-24} esu
β_{xxx}	98.6901 a.u.	89.4452 a.u.
β_{yyy}	-21.2734 a.u.	12.2380 a.u.
β_{xzz}	-92.0172 a.u.	-100.3622 a.u.
β_{yyy}	20.1007 a.u.	-84.7298 a.u.
β_{xxy}	-39.8584 a.u.	-88.3315 a.u.
β_{yzz}	-12.5972 a.u.	-41.7602 a.u.
β_{zzz}	-199.4366 a.u.	-273.5181 a.u.
β_{xxz}	209.2387 a.u.	236.7239 a.u.
β_{yyz}	-119.2180 a.u.	-167.8195 a.u.
$\langle\beta\rangle$	115.0298 a.u.	296.6763 a.u.
$\langle\beta\rangle$	993.7770×10^{-33} esu	$2563.0756 \times 10^{-33}$ esu

Table 4. The calculated total molecular energies, frontier orbital energies, electronegativity, hardness and softness for BTZA.

	HF/6-311++G(d,p)	B3LYP/6-311++G(d,p)
E_{HOMO} (eV)	-9.3638	-6.4037
E_{LUMO} (eV)	0.5197	-1.0514
$\Delta E = E_{LUMO} - E_{HOMO}$ (eV)	9.8835	5.3523
I (eV)	9.3638	6.4037
A (eV)	-0.5197	1.0514
χ (eV)	4.4221	3.7276
η (eV)	4.9418	2.6762
S (eV^{-1})	0.1113	0.1868
E_{TOTAL} (a.u)	-3325.8155	-3333.2019

The energy gap between the HOMO and LUMO characterizes the molecular chemical stability, chemical reactivity as well as hardness and softness of a molecule. B3LYP level predicts lower energy gap between HOMO and LUMO energies than HF level. By using HOMO and LUMO, energy values for a molecule, electronegativity and chemical hardness can be calculated as follows: $\chi = \frac{I+A}{2}$ (electronegativity), $\eta = \frac{I-A}{2}$ (chemical hardness) $S = \frac{1}{2\eta}$ (chemical softness) where I and A are the ionization potential and electron affinity, and $I = -E_{HOMO}$ and $A = -E_{LUMO}$, respectively [34]. In any two molecules, an electron will be transferred from the one of low χ to that of high χ (electrons flow from high chemical potential to low chemical potential). In the title compound, χ values were defined as 4.4221 and 3.7276 eV at HF and B3LYP levels. It has been reported that DFT calculations provide more accurate data than Hartree Fock model [35]. However, according to the total minimum energies calculated at HF and B3LYP levels, HF predicts lower minimum energy than B3LYP level. In other words, the molecular structure calculated at HF is more stable than the one calculated at B3LYP level.

Surfaces for the frontier orbitals were drawn to understand the bonding scheme of present compound. 3D plots of the second highest and the highest occupied MOs and the lowest and the second lowest unoccupied MOs, which are described as HOMO-1, HOMO, LUMO and LUMO+1 using DFT/B3LYP/6-311G(d,p) method, for the title compound are shown in Fig. 7.

3.6. Mulliken, Atomic Polar Tensor (APT), Natural (NBO) charge analysis

We calculated the molecular electrostatic potential (MESP) and the contour maps of molecular electrostatic potential surface and discussed their distributions. The 3D plot of MESP obtained using DFT/6-311++G(d,p) method for the title compound is given in Fig. 8.

It is clear that Mulliken [36] populations yield one of the simplest pictures of charge distribution and Mulliken charges render net atomic populations in the molecule. Atomic Polar Tensor

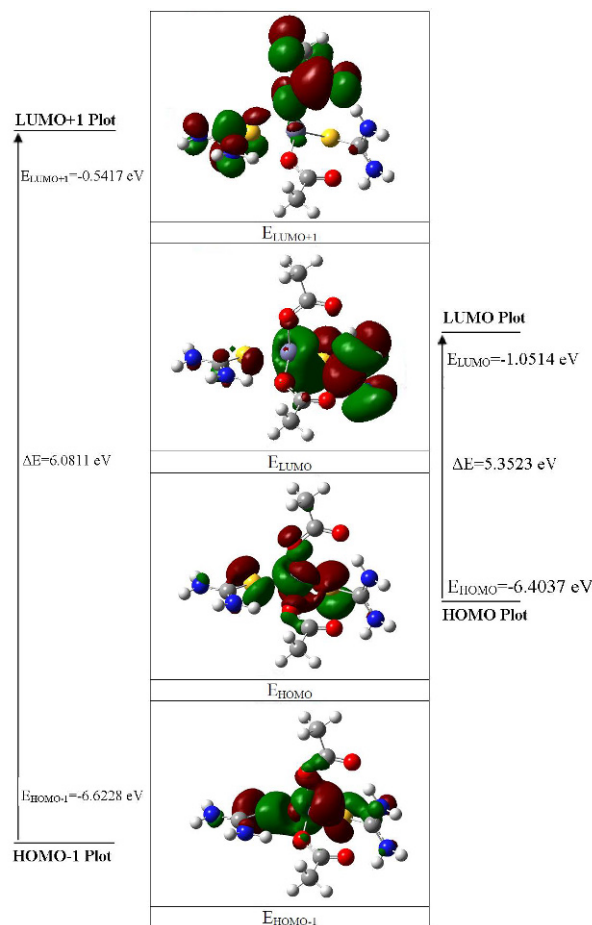


Fig. 7. 3D plots of frontier orbital energies for BTZA, obtained using B3LYP/6-311G(d,p) method.

(APT) is interpreted as a sum of charge tensor and charge flux tensor, leading to a charge-charge flux model [37]. The charge distribution of BTZA molecule has been calculated by the Mulliken and APT methods at HF/6-311++G(d,p) and B3LYP/6-311++G(d,p) levels of theory. Atomic natural bond orbital (NBO) charge distribution was also analyzed according to the results calculated with the same methods. The results are given in Table 5.

It follows from the calculation that the carbon atoms attached to oxygen and nitrogen atoms C1, C3, C5, and C6 exhibit more positive charges in comparison with the other carbon atoms in the molecule. Additionally, the triplet carbon atoms (C2 and C4) have the most negative charges due to the attached protons. In Fig. 9, Zn atom has pos-

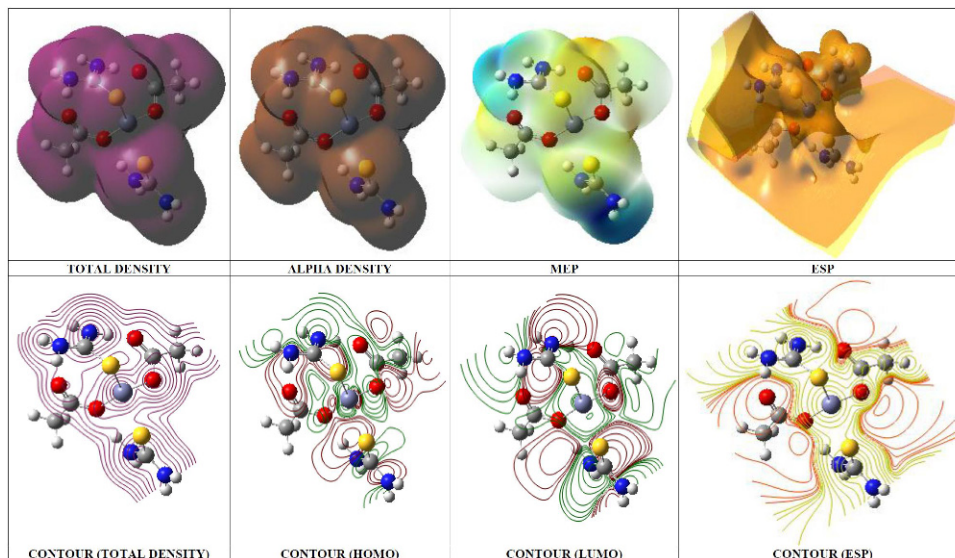


Fig. 8. Molecular surfaces of BTZA obtained at B3LYP/6-311++G(d,p) level.

Table 5. The Mulliken, APT and NBO charge distribution calculated (with 6-311++G(d,p)) for BTZA.

Atom	Mulliken		APT		NBO	
	HF	B3LYP	HF	B3LYP	HF	B3LYP
Zn	0.939286	0.794452	1.592450	1.439188	1.24256	1.03660
S ₁	-0.615236	-0.436498	-0.643676	-0.592572	-0.37421	-0.26949
S ₂	-0.676268	-0.529006	-0.703745	-0.621663	-0.32884	-0.20960
O ₂	-0.598838	-0.403050	-1.327831	-1.201487	-0.99008	-0.87897
O ₄	-0.371760	-0.183172	-1.280064	-1.114919	-0.94987	-0.82119
C ₁	0.559369	0.279169	1.475206	1.250129	0.96882	0.81416
C ₃	0.623195	0.328964	1.503282	1.268024	0.98415	0.82628
O ₁	-0.413041	-0.301234	-1.024569	-0.848378	-0.78035	-0.67803
O ₃	-0.547440	-0.418218	-1.127843	-0.981275	-0.82483	-0.72356
C ₂	-0.779043	-0.713334	-0.007424	-0.070385	-0.59403	-0.66383
C ₄	-0.703286	-0.668651	-0.008000	-0.075444	-0.59155	-0.65792
C ₅	0.039371	-0.135704	1.296873	1.132881	0.54708	0.37986
C ₆	0.324011	0.073954	1.392706	1.197675	0.49923	0.32831
N ₄	-0.370540	-0.244381	-0.892400	-0.786740	-0.81173	-0.77123
N ₃	-0.585455	-0.452698	-0.880232	-0.792373	-0.82117	-0.76666
N ₁	-0.405693	-0.312698	-0.893081	-0.817132	-0.80091	-0.73914
N ₂	-0.172610	-0.125098	-0.833849	-0.739157	-0.80303	-0.75429

itive charge, while S atoms have negative charges. As can be seen from the Table 4, the magnitudes of the carbon Mulliken charges, found to be either positive or negative, were noted to change from

-0.779043 to 0.939286 for the title compound. The Mulliken charges show a behavior similar to that of the APT and NBO charges. A comparison of Mulliken, APT and NBO plots of the ti-

the compound, calculated using HF/6-311++G(d,p) and B3LYP/6-311++G(d,p) basis sets, is shown in Fig. 9.

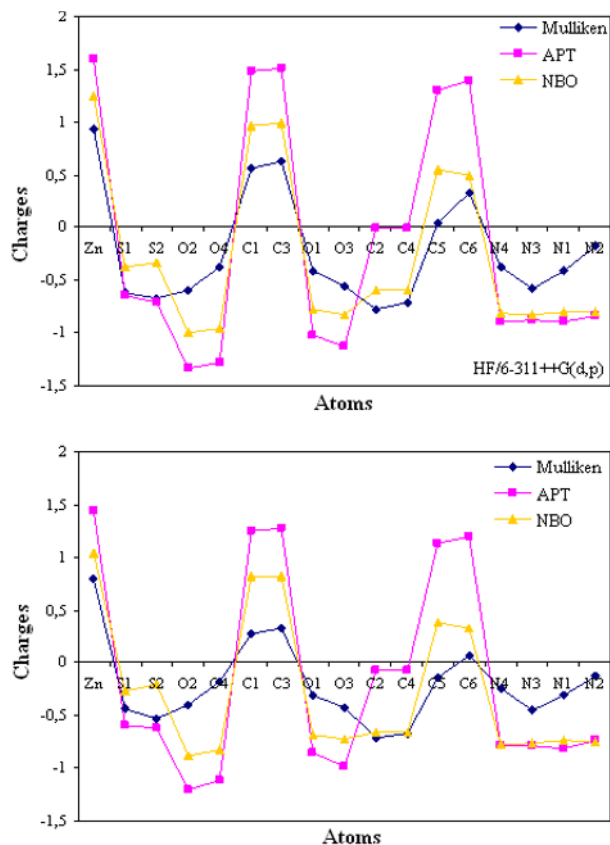


Fig. 9. Comparison of Mulliken, APT and NBO plots for BTZA, obtained with HF/6-311++G(d,p) and B3LYP/6-311++G(d,p) basis sets.

4. Conclusions

In this study, molecular structure, IR and Raman spectra, conformation study, Natural Bonding Orbital (NBO) analysis, HOMO and LUMO energy analysis, electronegativity (χ), hardness (η), softness (S), molecular electrostatic potential maps (MEP), Mulliken charges and atomic polar tensor-based charges, electric dipole moment (μ), polarizability (α) and the first-order hyperpolarizability (β), electronic and thermodynamic properties of BTZA molecule have been calculated by using HF/6-311++G(d,p) and B3LYP/6-311++G(d,p) methods. The obtained results for multiplication factors seem to be in a good agreement with exper-

imental data. In particular, the results obtained by B3LYP method seem to be better in evaluating vibrational frequencies in relation to the experimental data than those of HF. Likewise, B3LYP method seems to be more appropriate than HF method for the calculation of geometrical parameters of the molecules. The atomic charge results show that all the hydrogen atoms in the molecule have lost electrons and the results obtained at B3LYP and HF calculation levels are in good agreement with each other. Five possible conformers were obtained based on the PES scan method as a function of the dihedral angles, τ_1 (Zn-S₂-C₆-N₃), τ_2 (O₄-Zn-S₂-C₆), τ_3 (S₁-Zn-S₂-C₆), τ_4 (Zn-O₄-C₃-O₃) and τ_5 (O₂-Zn-O₄-C₃). The information about the size, shape, charge distribution and site of high electronegativity of the title compound has been obtained by mapping electron density isosurface with molecular electrostatic potential surfaces. NBO analysis has shown that the interaction energies of σ (C₅-N₁) \rightarrow π^* (C₅-N₁) and LP₁ (N₄) \rightarrow σ^* (C₆-N₃) result in intramolecular charge transfer, causing stabilization of the title compound. Additionally, from the calculated HOMO and LUMO energies, it can be seen that the charge transfer occurs in the compound. Our calculations show that all of the sulfur, nitrogen and oxygen atoms have negative charges, while hydrogen atoms have positive charges. From the NLO calculations, it can be concluded that the title compound can be used as an effective NLO material.

References

- [1] ANGELIMARY P.A., DHANUSKODI S., *Cryst. Res. Technol.*, 36 (2001), 1231.
- [2] USHASHREE P.M., MURALIDHARAN R., JAYAVEL R., RAMASAMY P., *J. Cryst. Growth*, 218 (2000), 365.
- [3] USHASHREE P.M., JAYAVEL R., SUBRAMANIAN C., RAMASAMY P., *J. Cryst. Growth*, 197 (1999), 216.
- [4] VENKATARAMANAN V., MAHESWARAN S., SHERWOOD J.N., BHAT H.L., *J. Cryst. Growth*, 179 (1997), 605.
- [5] RAJASEKARAN R., USHASHREE P.M., JAYAVEL R., RAMASAMY P., *J. Cryst. Growth*, 229 (2001), 563.
- [6] RAJASEKARAN R., KUMAR R.M., JAYAVEL R., RAMASAMY P., *J. Cryst. Growth*, 252 (2003), 317.
- [7] JAYALAKSHMI D., SANKAR R., JAYAVEL R., KUMAR J., *J. Cryst. Growth*, 276 (2005), 243.
- [8] JAYALAKSHMI D., KUMAR J., *Cryst. Res. Technol.*, 41 (2006), 37.

- [9] AVCI D., BASOĞLU A., ATALAY Y., *Int. J. Quant. Chem.* 111 (2011), 147.
- [10] AVCI D., *Spectrochim Acta A* 82 (2011), 37.
- [11] PIR H., GÜNAY N., AVCI D., ATALAY Y., *Spectrochim Acta A*, 96 (2012), 916.
- [12] TAMER Ö., SARIBOĞA B., UÇAR İ., BÜYÜKGÜNGÖR O., *Spectrochim Acta A*, 84 (2011), 168.
- [13] TAMER Ö., SARIBOĞA B., UÇAR İ., *Struct. Chem.*, 23 (2012), 659.
- [14] ATALAY Y., BASOĞLU A., AVCI, D., *Spectrochim. Acta A* 69 (2008), 460.
- [15] JAYALAKSHMI D., KESAVAMOORTHY R., THANGAVEL R., KUMAR J., *Physica B*, 371 (2006), 1.
- [16] BECKE A.D., *J. Chem. Phys.*, 98 (1993), 5648.
- [17] LEE C., YANG W., PARR R.G., *Phys. Rev. B* 37 (1988), 785.
- [18] Gaussian 09, Revision A.1, FRISCH M.J. et al., Gaussian, Inc., Wallingford CT, (2009).
- [19] GaussView, Version 5, DENNINGTON R., KEITH T., MILLAM J., Semichem Inc., Shawnee Mission KS, (2009).
- [20] SUNDARAGANESAN N., ILAKIAMANI S., SALEEM H., WOJCIECHOWSKI P.M., MICHALSKA D., *Spectrochim. Acta A*, 61 (2005), 2995.
- [21] REED A.E., CURTISS L.A., WEINHOLD F., *Chem. Rev.*, 88 (1988), 899.
- [22] CHOCHOLOUSOVA J., SPIRKO V.V., HOBZA P., *Phys. Chem. Chem. Phys.*, 6 (2004), 37.
- [23] ZHANG C.R., CHEM H.S., WANG G.H., *Chem. Res. Chin. Uni.*, 20 (2004), 640.
- [24] KUMAR P.S., *Spectrochim. Acta A*, 77 (2010), 45.
- [25] BUCKINGHAM A.D., *Chem. Phys.*, 12 (1967), 107.
- [26] CHRISTIANSEN O., GAUSS J., STANTON J. F., *Chem. Phys. Lett.*, 305 (1999), 147.
- [27] BLOEMBERGEN N., *Nonlinear optics*, Benjamin, New York, 1965.
- [28] LANE N.F., *Rev. Mod. Phys.*, 52 (1980), 29.
- [29] BIRNBAUM G., *Phenomena Induced by Intermolecular Interactions*, Plenum, New York, 1980.
- [30] MAROULIS G., *J. Chem. Phys.* 113 (2000), 5.
- [31] AVCI D., CÖMERT H., ATALAY Y., *J. Mol. Mod.*, 14 (2008), 161.
- [32] ATALAY Y., AVCI D., BAŞOĞLU A., *Struct. Chem.*, 19 (2008), 239.
- [33] FUKUI K., *Science* 218 (1982), 747.
- [34] PEARSON R.G., *Proceeding of the National Academy of Sciences*, 83 (1986), 8440
- [35] AVCI D., ATALAY Y., CÖMERT H., DIŇER M., *Arab. J. Sci. Eng.* 36 (2011) 607.
- [36] MULLIKEN R.S., *J. Chem. Phys.* 23 (1955), 1833.
- [37] MUKHERJEE V., SINGH N.P., YADAV R.A., *Spectrochim. Acta A*, 73 (2009), 249.

Received 2012-02-25

Accepted 2013-04-10